Advances in Nano Research, *Vol. 16, No. 5 (2024) 473-487*
https://doi.org/10.12989/anr.2024.16.5.473

Assessment of nonlocal nonlinear free vibration of bi-directional functionally-graded Timoshenko nanobeams

Elnaz Zare[1a], Daria K. Voronkova[2,3b], Omid Faraji[4c], Hamidreza Aghajanirefah[5a], Hamid Malek Nia[6c], Mohammad Gholami[1b] and Mojtaba Gorji Azandariani[*7,8]

[1]*Department of Civil Engineering, Yasouj University, Yasouj, Iran*
[2]*Department of Mathematics and Natural Sciences, Gulf University for Science and Technology, Mishref Campus, Kuwait*
[3]*Bauman Moscow State Technical University Moscow, Russia*
[4]*Department of Civil Engineering, Imam Hossein University, Tehran, Iran*
[5]*Department of Civil Engineering, Faculty of Engineering, Qazvin Branch Islamic Azad University, Qazvin, Iran*
[6]*Department of of Civil Engineering, Arak Branch, Islamic Azad University, Arak, Iran*
[7]*Department of Civil Engineering, Semnan University, Semnan, Iran*
[8]*Centre for Infrastructure Engineering, Western Sydney University, Sydney, Australia*

(*Received February 24 2023, Revised September 22, 2023, Accepted September 23, 2023*)

Abstract. The current study employs the nonlocal Timoshenko beam (NTB) theory and von-Kármán's geometric nonlinearity to develop a non-classic beam model for evaluating the nonlinear free vibration of bi-directional functionally-graded (BFG) nanobeams. In order to avoid the stretching-bending coupling in the equations of motion, the problem is formulated based on the physical middle surface. The governing equations of motion and the relevant boundary conditions have been determined using Hamilton's principle, followed by discretization using the differential quadrature method (DQM). To determine the frequencies of nonlinear vibrations in the BFG nanobeams, a direct iterative algorithm is used for solving the discretized underlying equations. The model verification is conducted by making a comparison between the obtained results and benchmark results reported in prior studies. In the present work, the effects of amplitude ratio, nanobeam length, material distribution, nonlocality, and boundary conditions are examined on the nonlinear frequency of BFG nanobeams through a parametric study. As a main result, it is observed that the nonlinear vibration frequencies are greater than the linear vibration frequencies for the same amplitude of the nonlinear oscillator. The study finds that the difference between the dimensionless linear frequency and the nonlinear frequency is smaller for CC nanobeams compared to SS nanobeams, particularly within the α range of 0 to 1.5, where the impact of geometric nonlinearity on CC nanobeams can be disregarded. Furthermore, the nonlinear frequency ratio exhibits an increasing trend as the parameter μ is incremented, with a diminishing dependency on nanobeam length (L). Additionally, it is established that as the nanobeam length increases, a critical point is reached at which a sharp rise in the nonlinear frequency ratio occurs, particularly within the nanobeam length range of 10 nm to 30 nm. These findings collectively contribute to a comprehensive understanding of the nonlinear vibration behavior of BFG nanobeams in relation to various parameters.

Keywords: bi-directional functionally-graded; differential quadrature method; Eringen's nonlocal theory; nanobeams; nonlinear vibration

1. Introduction

Due to the unique properties included in the functionally graded (FG) beams, including low density, high strength, thermal resistance, and toughness, they have attracted much attention among scholars and engineers (Aydogdu and Taskin 2007, Sina *et al*. 2009). Many research works have been conducted in the last few years on the different aspects included in FG beams (Aydogdu *et al*. 2018, Azandariani *et al*. 2022, Ebrahimi and Haghi 2018, Gholami *et al*. 2023, Luat *et al*. 2021). FGMs have been utilized in micro/nano-beams due to technological developments and achievements. Given the great potential of micro/ nanobeams in engineering applications, gaining a proper understanding of their mechanical behavior is of great importance. Due to the small-scale impacts at the nanoscale, classic continuum theories suffer from inaccurate predictions done for the mechanical behavior of nanostructures. In this regard, a few size-dependent elasticity mechanics have been developed, including nonlocal elasticity theory (Eringen 1983), modified couple stress (MCS) theory (Yang *et al*. 2002), and nonlocal strain gradient theory (Lim *et al*. 2015).

Due to technological developments and achievements, functionally graded materials have found their way into micro/nanobeams. Given the great potential of micro/ nanobeams in engineering applications, gaining a proper understanding of their mechanical behavior is of great importance. On the other hand, with the advance of nanotechnology, microbeams, whose thickness is generally on the order of microns and sub-microns, have been widely used in many applications of microdevices (Belarbi *et al*. 2021, Daikh *et al*. 2021, Hirane *et al*. 2021). Micro-electro-

*Corresponding author, Associate Professor,
E-mail: mgorji@semnan.ac.ir
[a] M.Sc.
[b] Assistant Professor
[c] Ph.D. Candidate

ISSN: 2287-237X (Print), 2287-2388 (Online)

mechanical systems are a technology that, in its most general form, can be defined as devices and structures made using microfabrication techniques in its most general form. The critical physical dimensions of micro-electro-mechanical systems devices can vary from well below one micron on the lower end of the dimensional spectrum, all the way to several millimeters (Elmascri *et al*. n.d., Karami *et al*. 2019a, b, 2020, Karami and Janghorban 2020, Rabhi *et al*. 2020, Xu *et al*. 2021). While the functional elements of micro-electro-mechanical systems are miniaturized structures, sensors, actuators, and microelectronics, the most notable elements are the microsensors and micro-actuators. However, it is experimentally proved that the size effect also becomes important for the mechanical behavior of microstructures when the dimensions of structures become on the order of microns and sub-microns. Due to this fact, it is inevitable to consider the size effect in analyzing the mechanical behavior of microstructures. At the same time, since controlled experiments in microscale are both difficult and expensive, the development of appropriate mathematical models for microstructures is an important issue concerning an approximate analysis of microstructures (Karami *et al*. 2018, 2019c, Karami and Janghorban 2019).

A large number of studies have focused on evaluating the buckling and vibration behavior of FG microbeams and nanobeams. For example, the MCS theory was utilized in a study to analyze the free vibration of FG Timoshenko microbeams (Asghari *et al*. 2011). In another study (Ansari *et al*. 2011), the free vibrations of FG microbeams were analyzed using the strain gradient Timoshenko beam theory. A group of researchers has evaluated the nonlinear free vibration of the FG microbeams using the MCS theory based on the von-Karman geometric nonlinearity (Eltaher *et al*. 2012). Utilizing the non-local Euler beam theory, a finite element formulation was proposed to analyze the free vibrations in the FG nanobeams (Eltaher *et al*. 2013a, b, Ke *et al*. 2012). In these works, the size-dependent static-buckling behavior in the FG nanobeams was also assessed using the nonlocal continuum model. In another work, the bending/buckling behaviors of FG nanobeam have been examined through an analytical approach concerning the non-local Timoshenko and Euler–Bernoulli beam theories (Simsek and Yurtcu 2013). In addition, the vibrations were also examined in the simply supported (SS) Timoshenko FG nanobeams applying the MCS theory (Rahmani and Pedram 2014). Through an analytical study, the size-dependent bending/ buckling behaviors were examined in the FG nanobeams considering the effects induced by thickness stretching (Chaht *et al*. 2015). Moreover, many other investigations have been performed on the vibrations and the buckling behavior of the FG micro/nanobeams (Ahouel *et al*. 2016, Atmane *et al*. 2015, Bennai *et al*. 2015, Chaht *et al*. 2015, Meradjah *et al*. 2015, Saidi *et al*. 2013, Zenkour and Abouelregal 2015).

Gao *et al*. (2019) investigated non-linear thermal buckling of bi-directional FG beams in the theoretical frameworks of nonlocal strain gradient theory. This study employed a higher-order shear deformation theory that incorporates a physical neutral surface to derive the size-dependent governing equations, combined with Hamilton's principle and the von Kármán geometric nonlinearity. Also, a parametric study is performed in detail after verifying the analysis, especially for the effects of nonlocal parameter, strain gradient length scale parameter, and the ratio of the them on the critical thermal buckling temperature of beams. Ebrahimi and Barati (2018) provide an analytical solution to the buckling governing equations of functionally graded piezoelectric (FGP) nanobeams obtained using a developed third-order shear deformation theory. Employing Hamilton's principle, the nonlocal governing equations of an FG nanobeam made of piezoelectric materials were obtained, and they were solved by applying a Navier-type analytical solution. Ebrahimi and Barati (2018) validated the present model's accuracy by comparing it with nonlocal Timoshenko FG beams. Aydogdu *et al*. (2018) studied the vibration of axially FG nano-rods and beams. The Ritz method with algebraic polynomials and stress gradient elasticity theory with the nonlocal effects formulated the problems. Also, the nonlocal parameter was assumed to change linearly or quadratically along the length of the nanostructure. Frequencies were compared to constant nonlocal parameter cases, and considerable differences were observed between constant and variable nonlocal parameter cases. Mode shapes in various cases are depicted to explain the effects of axial grading. Luat *et al*. (2021) investigated the bending, free vibration, and buckling analysis of a novel bi-functionally graded sandwich nanobeam via a nonlocal refined simple shear deformation theory. The novel sandwich beam included one ceramic core and two different FG face sheets. Eringen's nonlocal elasticity theory was utilized in cooperation with a refined simple shear deformation theory and Hamilton's principle to derive the equations of motion. A closed-form solution based on Navier's technique was used to solve the equations of motion of supported nanobeams. Also, in this study, the results were compared with existing solutions to evaluate the accuracy of the proposed theory. Zidi *et al*. (2017) proposed a novel simple higher-order shear deformation theory for bending and free vibration analysis of FG beams. In this method, equations of motion were obtained via Hamilton's principle. Zidi *et al*. (2017) analytical equations for the bending and free vibration analysis were presented for simply supported beams. In the final, the numerical results were compared with those of other higher-order shear deformation beam theories were obtained and validated.

Nonlinear vibration of beams under very large displacements is a major problem in the field of structural engineering. The beam vibration behavior is in nonlinear regime when the ends of a beam subjected to large transverse loads are axially immovable because of axial tension induced by a large deflection. Most recently, some authors have tried to evaluate the nonlinear behavior of FG structures (Ghorbanpour Arani *et al*. 2013, Hashemian *et al*. 2019, 2020, Moatallebi *et al*. 2022, Saffari *et al*. 2017). Through a study conducted on the nonlinear behavior in the FG structures, the size dependency of nonlinear vibrations has been investigated in the FG microbeams using the Casimir force, combined electrostatic force, and temperature changes (Jia *et al*. 2015). In another study, the non-linear bending behavior was investigated in the tapered FG beam subjected to the thermal/mechanical loads (Niknam *et al*. 2014). In a different work, an exact solution was proposed by some scholars to solve the nonlinear forced vibrations in the FG nanobeams by taking into account the surface effect (Ansari *et al*. 2015). The nonlinear vibrations of the size-dependent beam were investigated according to the Eringen's nonlocal elasticity theory using the von-Kármán geometric non- linearity (Şimşek 2014). In addition to the mentioned investigations, some other investigations have been performed on the nonlinear free vibration of FG micro/nanobeams (Almitani *et al*. 2021, Amar *et al*. 2017, Gao *et al*. 2019, Kim *et al*. 2014, Nejad *et al*. 2018, Sanjay Anandrao *et al*. 2012, Setoodeh and Rezaei 2017, Zidi *et al*. 2017).

Nanotechnology has prominent advantages for developers who are working to make people's lives easier. This relatively new technology has led to the construction of subatomic or nanostructured structures that have a variety of applications in medicine, electronics, mechanics, solar cells, etc. Therefore, in the field of mechanical engineering, the study of the behavior of nanoscale structures has been of great importance. Three different methods are suggested to predict the mechanics of these structures (i.e., experimental tests, molecular dynamics (MD) simulation, and non-classical theories). Experimental tests and MD simulations have more complexity compared to non-classical theories, which has led to the development of this category of theories in recent years. Because in engineering, reducing the complexity of computing, which leads to time and cost savings, is important.

A review of the history of the above research clearly shows that no attention has been paid to the mechanical behavior of nanobeams with geometric nonlinearity and to the author's knowledge, no published work on eringen's nonlocal theory for non-linear free vibration of bi-directional functionally graded Timoshenko nanobeams there is no pair. Accordingly, in the present study, the impact of the nonlinearity related to geometry is thoroughly examined on the free vibration of BFG nanobeams applying Eringen's nonlocal theory. In order to simplify the formulation, the problem formulas are derived according to the physical middle surface. The Hamilton principle is employed to determine governing partial differential equations as well as boundary conditions. Moreover, the dynamic stiffness method (DSM) and direct iterative method are applied to solve governing equations. Present results for non-linear static deflection were compared with previously published results in order to validate the present formulation. The impacts of the nonlocal factors, beam length and material property gradient on the non-linear free vibration of BFG nanobeams are investigated. It is observed that these parameters are vital in the value of the non-linear free vibration of the BFG nanobeam.

As far as the authors know, there have been no studies evaluating the mechanical behavior of the BFG nanobeams with geometric nonlinearity. Accordingly, in the present study, the effect of geometric nonlinearity is thoroughly examined on the free vibration properties in the BFG nanobeams applying the Eringen's nonlocal theory. The remainder of this article is organized as follows: the next section deals with BFG materials and Eringen's nonlocal theory. Section 3 deals with the determination of non-local nonlinear underlying equations and corresponding boundary conditions according to the Timoshenko beam theory. Section 4 deals with the use of GDQM to solve the resulted equations in Section 3. Section 5 deals with the parametric study on the effect of amplitude ratio, nanobeam length, material distribution, nonlocal parameter, and boundary conditions on the nonlinear vibration frequencies in BFG nanobeams. Finally, the paper concludes with Section 6.

2. Theoretical formulation

The mechanical characteristics of FG beams gradually change along their thickness directions, while the material characteritics of bi-directional FG beams change along both the beam's length and thickness (Fig. 1(a)). An important point that must be mentioned here is that the above-mentioned studies focus on FG micro/nanobeams. The findings available from previous studies on BFG micro/nanobeams are not considerable. In a few studies on the BFG nanobeams considering the buckling, bending, and vibration behaviors, the Eringen's nonlocal theory was developed using the differential quadrature method (DQM) according to the Euler–Bernoulli theory (Nejad 2016, Nejad *et al*. 2016, Nejad and Hadi 2016a). The buckling and vibration behaviors were also analyzed in the BFG porous tapered micro/nanobeams and imperfect BFG porous micro/nanobeams applying the Euler–Bernoulli beam theory and the Timoshenko beam theory, respectively (Dergachova and Zou 2021, Nejadi and Mohammadimehr 2020, Zhou *et al*. 2022).

2.1 Functionally-graded materials

Suppose a BFG nanobeam has a length of L and a rectangular cross-section defined as $b \times h$ (where b is the width and h is the height), while it has immovable simple supports at both ends (Fig. 1(b)). In order to simplify the calculations, Poisson's ratio ν is assumed as constant. Moreover, the following equations give mass density ρ and Young's modulus E (Nejad and Hadi 2016b):

$$E(x, z_{ms}) = e^{N_x \frac{x}{L}} \left[(E_c - E_m) \left(\frac{z_{ms}}{h} + \frac{1}{2} \right)^{N_z} + E_m \right] \quad (1)$$

$$\rho(x, z_{ms}) = e^{N_x \frac{x}{L}} \left[(\rho_c - \rho_m) \left(\frac{z_{ms}}{h} + \frac{1}{2} \right)^{N_z} + \rho_m \right] \quad (2)$$

where m is the metallic constituent, c is the ceramic constituent, N_x and N_z indicate the gradient parameters dictating the material variation profile along the thickness direction and length direction of the nanobeam, respectively.

An important point here is that in Eq. (1), the geometric mid-surface z_{ms} is considered as a reference for the material characteristics. As is known, the geometric mid-surface may

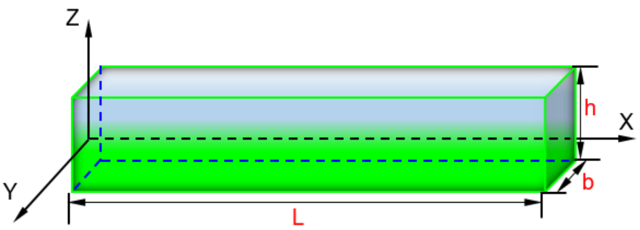

(a)

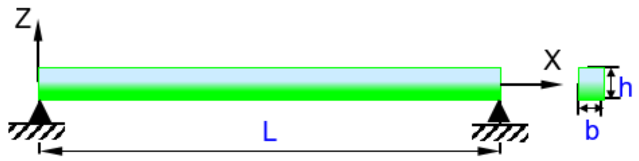

(b)

Fig. 1 Bi-directional functionally graded (BFG) nanobeam: (a) variation in mechanical properties, and (b) physical neutral surface and geometric mid-surface

not coincide with the neutral surface in the BFG nanobeams in cases where the material characteristics of the BFG nanobeam are asymmetric about its geometric mid-surface, resulting in stretching and bending coupling to develop. However, stretching and bending coupling will be disappeared, provided that the position of the physical neutral surface is identified, and then the coordinate system's origin is set to the physical neutral surface (Fig. 1(b)).

The relationship between the geometric mid-surface and physical neutral surface is expressed as follows (Şimşek 2016):

$$z_{ms} = z_c + e\,, \qquad e = \frac{\int_{-\frac{h}{2}}^{\frac{h}{2}} E(z_{ms})dz_{ms}}{\int_{-\frac{h}{2}}^{\frac{h}{2}} dz_{ms}} \tag{3}$$

when the physical neutral surface is considered as the reference, the material properties (Eqs. (1) and (2)) take the form presented in Eqs. (4) and (5).

$$\boldsymbol{E(x, z_c) = e^{N_x \frac{x}{L}}\left[(E_c - E_m)\left(\frac{z_c + e}{h} + \frac{1}{2}\right)^{N_z} + E_m\right]} \tag{4}$$

$$\boldsymbol{\rho(x, z_c) = e^{N_x \frac{x}{L}}\left[(\rho_c - \rho_m)\left(\frac{z_c + e}{h} + \frac{1}{2}\right)^{N_z} + \rho_m\right]} \tag{5}$$

2.2 Eringen's nonlocal theory

Eringen's nonlocal theory (Eringen 1983) assumes that the stress tensor at any point *x* within the material domain is influenced by two different factors: **(i)** the strain tensor at x, and **(ii)** the strain tensor at all the other points within the domain, which is consistent with experimental data reported in the literature based on the atomic theory and lattice dynamics in phonon scattering. Based on this theory,

The following equations can be utilized for defining the components of the nonlocal stress-tensor $\sigma_{ij}(x)$ at any point x in the homogeneous elastic body:

$$\boldsymbol{\sigma_{ij}(x) = \int_{\Omega}^{l} \alpha(|x' - x|\,, \tau) t_{ij}(x') d\Omega(x')} \tag{6}$$

where $t_{ij}(x')$ is the component for the classic local stress-tensor at point x. A relationship can be defined between classic local stress-tensor, and the linear strain tensor ε_{kl} using the underlying equations for a Hookean material:

$$\boldsymbol{t_{ij} = c_{ilkl}\varepsilon_{kl}} \tag{7}$$

In Eq. (6) α is the kernel function known as nonlocal modulus, which depends on two variables $|x' - x|$ defined as the distance in Euclidean form and τ that is determined as follows:

$$\boldsymbol{\tau = \frac{e_0 a}{l}} \tag{8}$$

where τ represents the ratio of a characteristic internal length a (e.g., granular distance, lattice parameter) to a characteristic external length l (e.g., wavelength, crack length), which is related to each material using an adjusting constant, e_0. The e_0 magnitude is estimated through two ways: **(i)** by fitting the dispersion curves of plane waves to the dispersion curves of atomic lattice dynamics or, **(ii)** experimentally.

According to study conducted by Eringen (1983), the integral form of the non-local constitutive equation (Eq. (6)) can be expressed in differential form in the following way if the appropriate kernels function is chosen:

$$\boldsymbol{(1 - (e_0 a)^2 \nabla^2)\sigma_{kl} = t_{kl}} \tag{9}$$

where ∇^2 indicates the Laplacian operator. For one dimension, it is possible to simplify the non-local constitutive relation (Eq. (9)) for an elastic material as follows:

$$\boldsymbol{\sigma_{xx} - (e_0 a)^2 \frac{\partial^2 \sigma_{xx}}{\partial x^2} = E\varepsilon_{xx}} \tag{10a}$$

$$\boldsymbol{\sigma_{xz} - (e_0 a)^2 \frac{\partial^2 \sigma_{xz}}{\partial x^2} = G\gamma_{xz}} \tag{10b}$$

where E denotes the elasticity modulus, G denotes the shear modulus, σ_{xx} denotes the normal axial stress, σ_{xz} denotes the shear stress, ε_{xx} denotes the axial strain, and γ_{xz} denotes the shear strain.

3. Basic equations and boundary conditions

The current analysis utilizes the Timoshenko beam theory. Thus, the The displacements u_1, u_2 and u_3 along directions of X, Y and Z for any point of the micro beam are determined by (Rahmani and Pedram 2014):

$$\begin{aligned} &\boldsymbol{u_1(x,z,t) = u(x,t) - z_c\phi(x,t)} \\ &\boldsymbol{u_2(x,z,t) = 0} \\ &\boldsymbol{u_3(x,z,t) = w(x,t)} \end{aligned} \tag{11}$$

where $w(x,t)$ and $u(x,t)$ are the transverse and axial displacements of a point on the beam mid-plane along the X and Z directions, respectively. Moreover, t denotes the time and $\phi(x,t)$ denotes the bending rotation of the crosssections. In the Timoshenko beam theory, the nonzero strains can be expressed as follows (Li *et al*. 2016):

$$\begin{aligned}\boldsymbol{\varepsilon_{xx}} &= \frac{\partial \boldsymbol{u}}{\partial \boldsymbol{x}} + \frac{\mathbf{1}}{\mathbf{2}}\left(\frac{\partial \boldsymbol{w}}{\partial \boldsymbol{x}}\right)^{2} - \boldsymbol{z_c}\frac{\partial \boldsymbol{\phi}}{\partial \boldsymbol{x}}\\ \boldsymbol{\varepsilon_{xz}} &= \frac{\mathbf{1}}{\mathbf{2}}\left(\frac{\partial \boldsymbol{w}}{\partial \boldsymbol{x}} - \boldsymbol{\phi}\right)\end{aligned} \tag{12}$$

The strain energy U corresponding to the BFG nano-beams is determined by the use of Eq. (12) as follows (Li *et al*. 2016):

$$\begin{aligned}U &= \frac{1}{2}\int_0^L\int_A^d(\sigma_{xx}\,\varepsilon_{xx} + 2\sigma_{xz}\varepsilon_{xz})dAdx\\ U &= \frac{1}{2}\int_0^L h\begin{bmatrix} N_{xx}\left(\dfrac{\partial u}{\partial x} + \dfrac{1}{2}\left(\dfrac{\partial w}{\partial x}\right)^2\right)\\ -M_{xx}\dfrac{\partial \theta}{dx} + Q_{xz}\left(\dfrac{\partial w}{\partial x} - \emptyset\right)\end{bmatrix}dx\end{aligned} \tag{13}$$

where N_{xx} denotes the resultant normal force, Q_x denotes the shear force, and M_{xx} denotes the bending moment. These can be expressed as:

$$\begin{aligned}&\boldsymbol{N_{xx}} = \int_A \boldsymbol{\sigma_{xx}dA}, \quad \boldsymbol{M_{xx}} = \int_A \boldsymbol{z_c\sigma_{xx}dA}\\ &\boldsymbol{Q_{xz}} = \int_A \boldsymbol{\sigma_{xz}dA}\end{aligned} \tag{14}$$

Considering both longitudinal displacement and transverse displacement, the kinetic energy of the system can be estimated as follows:

$$\begin{aligned}T &= \frac{1}{2}\int_0^L\int_A^d P(x.z)\left[\left(\frac{\partial u_1}{\partial t}\right)^2 + \left(\frac{\partial u_3}{\partial t}\right)^2\right]dAdx\\ &= \frac{1}{2}\int_0^L\left[I_0 e^{B\frac{x}{L}}\left(\left(\frac{\partial w}{\partial t}\right)^2 + \left(\frac{\partial u}{\partial t}\right)^2\right) + I_2 e^{B\frac{x}{L}}\left(\frac{\partial \emptyset}{\partial t}\right)^2\right]dx\end{aligned} \tag{15}$$

where:

$$\begin{aligned}&(I_0, I_2)\\ &= b\int_{-\frac{h}{2}-e}^{\frac{h}{2}-e}(1, z_c^2)\left[(\rho_c - \rho_m)\left(\frac{z_c + e}{h} + \frac{1}{2}\right)^{N_z} + \rho_m\right]dz\end{aligned} \tag{16}$$

Furthermore, as the integration is done based on the position of the physical neutral surface, The coefficient of coupling inertia will become zero, i.e., $\mathrm{I}_1 = \int_{-\frac{h}{2}-e}^{\frac{h}{2}-e} \mathrm{z_c}\left[(\rho_c - \rho_m)\left(\frac{z_c+e}{h} + \frac{1}{2}\right)^{N_z} + \rho_m\right]dz = 0$ (Şimşek 2016).

The Hamilton's principle is expressed below:

$$\delta\int_{t_1}^{t_2}(\mathrm{T} - \mathrm{U})\mathrm{dt} = 0 \tag{17}$$

The governing equations are determined through substituting the expressions for U (in Eq. (13)) and T (in Eq. (15)) into Eq. (17), performing a partial integration with respect to x and t, and finally using the fundamental lemma of the calculus of variations as follows:

$$\boldsymbol{\delta_u} \Rightarrow \frac{\partial \boldsymbol{N_{xx}}}{\partial \boldsymbol{x}} = \boldsymbol{I_0}\boldsymbol{e}^{\boldsymbol{B}\frac{x}{L}}\ \frac{\partial^2 \boldsymbol{u}}{\partial \boldsymbol{t}^2} \tag{18a}$$

$$\boldsymbol{\delta_\phi} \Rightarrow \boldsymbol{Q_{xz}} - \frac{\partial \boldsymbol{M_{xx}}}{\partial \boldsymbol{x}} = \boldsymbol{I_2}\boldsymbol{e}^{\boldsymbol{B}\frac{x}{L}}\ \frac{\partial^2 \boldsymbol{\phi}}{\partial \boldsymbol{t}^2} \tag{18b}$$

$$\boldsymbol{\delta_w} \Rightarrow \frac{\partial \boldsymbol{Q_{xx}}}{\partial \boldsymbol{x}} + \frac{\partial}{\partial \boldsymbol{x}}\left(\boldsymbol{N_{xx}}\frac{\partial \boldsymbol{w}}{\partial \boldsymbol{x}}\right) = \boldsymbol{I_0}\boldsymbol{e}^{\boldsymbol{B}\frac{x}{L}}\ \frac{\partial^2 \boldsymbol{w}}{\partial \boldsymbol{t}^2} \tag{18c}$$

A similar approach can be applied to develop the related boundary conditions (at X= 0 and L), as expressed below:

$$\boldsymbol{\delta_u} \Rightarrow \boldsymbol{N_{xx}} = \mathbf{0} \quad \boldsymbol{or} \quad \boldsymbol{u} = \mathbf{0} \tag{19a}$$

$$\boldsymbol{\delta_w} \Rightarrow \boldsymbol{Q_{xx}} + \boldsymbol{N_{xx}}\frac{\partial \boldsymbol{w}}{\partial \boldsymbol{x}} \quad \boldsymbol{or} \quad \boldsymbol{w} = \mathbf{0} \tag{19b}$$

$$\boldsymbol{\delta_\phi} \Rightarrow \boldsymbol{M_{xx}} = \mathbf{0} \quad \boldsymbol{or} \quad \boldsymbol{\phi} = \mathbf{0} \tag{19c}$$

As usual, it is possible to neglect the fast dynamics for the axis dynamics $\left(\frac{\partial^2 \boldsymbol{u}}{\partial \boldsymbol{t}^2} = \mathbf{0}\right)$ (Ke *et al*. 2012, Li and Hu 2016, Rahmani and Pedram 2014, Şimşek 2016).

By neglecting the axial inertia in Eq. (18a), one obtains $\boldsymbol{N_{xx}} = \boldsymbol{C}$, where C is a constant.

Using this relation ($\boldsymbol{N_{xx}} = \boldsymbol{C}$) and Eq. (18c), the following equation can be obtained:

$$\frac{\partial \boldsymbol{Q_{xx}}}{\partial \boldsymbol{x}} + \boldsymbol{N_{xx}}\frac{\partial^2 \boldsymbol{w}}{\partial \boldsymbol{x}^2} = \boldsymbol{I_0}\boldsymbol{e}^{\boldsymbol{B}\frac{x}{L}}\ \frac{\partial^2 \boldsymbol{w}}{\partial \boldsymbol{t}^2} \tag{20}$$

It is possible to determine the force-displacement and moment-displacement equations of the nonlocal Timoshenko beam theory using Eqs. (10a), (10b), (12) and (14) in the following:

$$\begin{aligned}&\boldsymbol{N_{xx}} - \mu\frac{\partial^2 \boldsymbol{N_{xx}}}{\partial \boldsymbol{x}^2}\\ &= \int_A \boldsymbol{E}(\boldsymbol{x}, \boldsymbol{z_c})\left[\frac{\partial \boldsymbol{u}}{\partial \boldsymbol{x}} + \frac{\mathbf{1}}{\mathbf{2}}\left(\frac{\partial \boldsymbol{w}}{\partial \boldsymbol{x}}\right)^2 - \boldsymbol{z_c}\frac{\partial^2 \boldsymbol{w}}{\partial \boldsymbol{x}^2}\right]\boldsymbol{dA}\\ &= \boldsymbol{A_0}\,\boldsymbol{e}^{\boldsymbol{B}\frac{x}{L}}\left[\frac{\partial \boldsymbol{u}}{\partial \boldsymbol{x}} + \frac{\mathbf{1}}{\mathbf{2}}\left(\frac{\partial \boldsymbol{w}}{\partial \boldsymbol{x}}\right)^2\right]\end{aligned} \tag{21a}$$

$$\begin{aligned}&\boldsymbol{Q_{xz}} - \mu\frac{\partial^2 \boldsymbol{Q_{xz}}}{\partial \boldsymbol{x}^2} = \int_A \boldsymbol{G}(\boldsymbol{x}, \boldsymbol{z_c})\left(\frac{\partial \boldsymbol{w}}{\partial \boldsymbol{x}} - \boldsymbol{\phi}\right)\boldsymbol{dA}\\ &= \boldsymbol{A_3}\,\boldsymbol{e}^{\boldsymbol{B}\frac{x}{L}}\left(\frac{\partial \boldsymbol{w}}{\partial \boldsymbol{x}} - \boldsymbol{\phi}\right)\end{aligned} \tag{21b}$$

$$\begin{aligned}&\boldsymbol{M_{xx}} - \mu\frac{\partial^2 \boldsymbol{M_{xx}}}{\partial \boldsymbol{x}^2}\\ &= \int_A \boldsymbol{E}(\boldsymbol{x}, \boldsymbol{z_c})\left[\boldsymbol{z_c}\frac{\partial \boldsymbol{u}}{\partial \boldsymbol{x}} + \frac{\mathbf{1}}{\mathbf{2}}\boldsymbol{z_c}\left(\frac{\partial \boldsymbol{w}}{\partial \boldsymbol{x}}\right)^2 - \boldsymbol{Z_c^2}\frac{\partial \boldsymbol{\phi}}{\partial \boldsymbol{x}}\right]\boldsymbol{dA}\\ &= -\boldsymbol{A_2}\boldsymbol{e}^{\boldsymbol{B}\frac{x}{L}}\ \frac{\partial \boldsymbol{\phi}}{\partial \boldsymbol{x}}\end{aligned} \tag{21c}$$

where the stiffness coefficients are expressed as follows:

$$\begin{aligned}&(A_0, A_2)\\ &= b\int_{-\frac{h}{2}-e}^{\frac{h}{2}-e}(1, z_c^2)\begin{bmatrix}(E_c - E_m)\left(\dfrac{z_c + e}{h} + \dfrac{1}{2}\right)^{N_z}\\ +E_m\end{bmatrix}dz\end{aligned} \tag{22a}$$

$$\mathrm{A_3} = \frac{\mathrm{bK_s}}{2(1+\mathrm{v})}\int_{-\frac{h}{2}-e}^{\frac{h}{2}-e}\left[(\mathrm{E_c}\text{-}\mathrm{E_m})\left(\frac{\mathrm{z_c}+\mathrm{e}}{\mathrm{h}} + \frac{1}{2}\right)^{\mathrm{N_z}} + \mathrm{E_m}\right]\mathrm{dz} \tag{22b}$$

It is worth noting that the stiffness coefficient, leading to the coupled stretching-bending problem, gets zero i.e. $A_1 = b\int_{-\frac{h}{2}-e}^{\frac{h}{2}-e} z_c\left[(E_c - E_m)\left(\frac{z_c+e}{h}+\frac{1}{2}\right)^{N_z} + E_m\right]dz = 0$.

The axial force (Eq. (21a)), shear force (Eq. (21b)), and moment (Eq. (21c)) can be expressed in the following way given to the fact that the axial force is constant and by the use of size-dependent equilibrium Eqs. (18c) and (20):

$$\boldsymbol{N_{xx}} = \boldsymbol{A_0}\ \boldsymbol{e^{B\frac{x}{L}}}\left[\frac{\partial \boldsymbol{u}}{\partial \boldsymbol{x}} + \frac{\boldsymbol{1}}{\boldsymbol{2}}\left(\frac{\partial \boldsymbol{w}}{\partial \boldsymbol{x}}\right)^2\right] = \boldsymbol{C} \tag{23a}$$

$$\begin{aligned}\boldsymbol{Q_{xz}} = \mu\Bigg[&\boldsymbol{I_0}\ \boldsymbol{e^{B\frac{x}{L}}}\ \frac{\partial^3 \boldsymbol{w}}{\partial \boldsymbol{x}\partial \boldsymbol{t}^2} + \frac{\boldsymbol{B}}{\boldsymbol{L}}\boldsymbol{I_0}\ \boldsymbol{e^{B\frac{x}{L}}}\ \frac{\partial^2 \boldsymbol{w}}{\partial \boldsymbol{t}^2} - \\ &\left(\boldsymbol{A_0}\ \boldsymbol{e^{B\frac{x}{L}}}\left[\frac{\partial \boldsymbol{u}}{\partial \boldsymbol{x}} + \frac{\boldsymbol{1}}{\boldsymbol{2}}\left(\frac{\partial \boldsymbol{w}}{\partial \boldsymbol{x}}\right)^2\right]\right)\frac{\partial^3 \boldsymbol{w}}{\partial \boldsymbol{x}^3}\Bigg] + \\ &\boldsymbol{A_3}\,\boldsymbol{e^{B\frac{x}{L}}}\left(\frac{\partial \boldsymbol{w}}{\partial \boldsymbol{x}} - \boldsymbol{\phi}\right)\end{aligned} \tag{23b}$$

$$\begin{aligned}\boldsymbol{M_{xx}} = \mu\Bigg[&\boldsymbol{I_0}\ \boldsymbol{e^{B\frac{x}{L}}}\ \frac{\partial^2 \boldsymbol{w}}{\partial \boldsymbol{t}^2} - \boldsymbol{I_2}\ \boldsymbol{e^{B\frac{x}{L}}}\ \frac{\partial^3 \boldsymbol{\phi}}{\partial \boldsymbol{x}\partial \boldsymbol{t}^2} - \\ &\frac{\boldsymbol{B}}{\boldsymbol{L}}\boldsymbol{I_2}\ \boldsymbol{e^{B\frac{x}{L}}}\ \frac{\partial^2 \boldsymbol{\phi}}{\partial \boldsymbol{t}^2} - \\ &\left(\boldsymbol{A_0}\ \boldsymbol{e^{B\frac{x}{L}}}\left[\frac{\partial \boldsymbol{u}}{\partial \boldsymbol{x}} + \frac{\boldsymbol{1}}{\boldsymbol{2}}\left(\frac{\partial \boldsymbol{w}}{\partial \boldsymbol{x}}\right)^2\right]\right)\frac{\partial^2 \boldsymbol{w}}{\partial \boldsymbol{x}^2}\Bigg] - \boldsymbol{A_2}\boldsymbol{e^{B\frac{x}{L}}}\ \frac{\partial \boldsymbol{\phi}}{\partial \boldsymbol{x}}\end{aligned} \tag{23c}$$

The nonlinear equations of motion can be determined using Eqs. (23a), (23b) and (23c):

$$\frac{\boldsymbol{B}}{\boldsymbol{L}}\left(\frac{\partial \boldsymbol{u}}{\partial \boldsymbol{x}} + \frac{\boldsymbol{1}}{\boldsymbol{2}}\left(\frac{\partial \boldsymbol{w}}{\partial \boldsymbol{x}}\right)^2\right) + \left(\frac{\partial^2 \boldsymbol{u}}{\partial \boldsymbol{x}^2} + \frac{\partial \boldsymbol{w}}{\partial \boldsymbol{x}}\frac{\partial^2 \boldsymbol{w}}{\partial \boldsymbol{x}^2}\right) = \boldsymbol{0} \tag{24a}$$

$$\begin{aligned}&\boldsymbol{\mu}\left(\left(\frac{\boldsymbol{B}}{\boldsymbol{L}}\right)^2\boldsymbol{I_2}\frac{\partial^2 \boldsymbol{\phi}}{\partial \boldsymbol{t}^2} + \boldsymbol{I_2}\frac{\partial^4 \boldsymbol{\phi}}{\partial \boldsymbol{x}^2\partial \boldsymbol{t}^2} + \boldsymbol{2}\frac{\boldsymbol{B}}{\boldsymbol{L}}\boldsymbol{I_2}\frac{\partial^3 \boldsymbol{\phi}}{\partial \boldsymbol{x}\partial \boldsymbol{t}^2}\right) + \\ &\boldsymbol{A_2}\frac{\partial^2 \boldsymbol{\phi}}{\partial \boldsymbol{x}^2} + \frac{\boldsymbol{B}}{\boldsymbol{L}}\boldsymbol{A_2}\ \frac{\partial \boldsymbol{\phi}}{\partial \boldsymbol{x}} + \boldsymbol{A_3}\left(\frac{\partial \boldsymbol{w}}{\partial \boldsymbol{x}} - \boldsymbol{\phi}\right) = \boldsymbol{0}\end{aligned} \tag{24b}$$

$$\begin{aligned}&\boldsymbol{A_3}\left(\frac{\partial^2 \boldsymbol{w}}{\partial \boldsymbol{x}^2} - \frac{\partial \boldsymbol{\phi}}{\partial \boldsymbol{x}}\right) + \frac{\boldsymbol{B}}{\boldsymbol{L}}\boldsymbol{A_3}\left(\frac{\partial \boldsymbol{w}}{\partial \boldsymbol{x}} - \boldsymbol{\phi}\right) + \\ &\boldsymbol{A_0}\left[\frac{\partial \boldsymbol{u}}{\partial \boldsymbol{x}} + \frac{\boldsymbol{1}}{\boldsymbol{2}}\left(\frac{\partial \boldsymbol{w}}{\partial \boldsymbol{x}}\right)^2\right]\left(\boldsymbol{1} - \mu\frac{\partial^2}{\partial \boldsymbol{x}^2}\right)\frac{\partial^2 \boldsymbol{w}}{\partial \boldsymbol{x}^2} - \\ &\left(\boldsymbol{1} - \mu\left(\frac{\boldsymbol{B}}{\boldsymbol{L}}\right)^2 - \mu\frac{\partial^2}{\partial \boldsymbol{x}^2} - 2\mu\frac{\boldsymbol{B}}{\boldsymbol{L}}\frac{\partial}{\partial \boldsymbol{x}}\right)\left(\boldsymbol{I_0}\ \frac{\partial^2 \boldsymbol{w}}{\partial \boldsymbol{t}^2}\right) = \boldsymbol{0}\end{aligned} \tag{24c}$$

As compared to the classical model of the Timoshenko beam, the orders of the nonlinear equations of motion are higher in the present model of BFG Timoshenko nanobeam (Su and Banerjee 2015). On the other hand, the equations developed by Li and Hu (2016) can be obtained when the effects of nonlocal parameter μ and parameter N_x are both neglected in Eqs. (24a)-(24c). Also, the equations developed by Li and Hu (2016) can be recovered by neglecting both effects of nonlinear terms and parameter N_x in Eqs. (24a) to (24c).

4. Analysis and solution process

The DQM method is frequently employed for solving the underlying differential equations with corresponding boundary conditions, for which it is hard to find analytical solutions. Here, the DQM method is used to solve Eqs. (24a) and (24b). First of all, in this section, a review is provided on the method.

The main function of this method involves estimating the derivatives of a dependent variable using a weighted linear combination of variable amounts at the nodes (predefined points within the domain). Consider a continuous function on x (f(x)) over 1D domain ($0 \leqslant X \leqslant L$), which can be expressed using Lagrange interpolation with predefined N points.

$$\begin{aligned}&\mathrm{f}(x) = \sum_{j=1}^{N} L_j(x)f_j \ \text{ for } \mathrm{j} = 1,2,\dots,\mathrm{N} \\ &\text{with } f_j = \mathrm{f}(x_j) \qquad \text{and } x_j \in [0, L]\end{aligned} \tag{25}$$

where $L_j(x)$ indicates the Lagrange interpolating function and f_j is the functional value corresponding to the jth node. Thus, the approximation of the n$^{\text{th}}$ derivative of the function is given by:

$$\begin{aligned}&f_i^{(n)} = \sum_{j=1}^{N} c_{ij}^{(n)}(x)f_i \ \text{ for } \mathrm{i} = 1,\dots\dots,\mathrm{N} \\ &\text{with } f_i^{(n)} = \left.\frac{d^n f(x)}{dx^n}\right|_{x=x_i}\end{aligned} \tag{26}$$

where $c_{ij}^{(n)}$ indicates the weight coefficient, representing the contribution of the functional value at the j$^{\text{th}}$ node to the n$^{\text{th}}$ derivative value at the i$^{\text{th}}$ node. The relations below give the weight coefficient:

For the first-order derivative($n = 1$) (Gorji Azandariani *et al.* 2022):

$$\begin{aligned}&c_{ij}^{(1)} = \frac{M(x_i)}{(x_i - x_j)M(x_j)}: \\ &\mathrm{i},\mathrm{j} = 1,2,\dots,\mathrm{n} \quad \text{and} \quad \mathrm{i} \neq \mathrm{j} \\ &c_{ij}^{(1)} = -\sum_{\substack{j=1\\ j\neq i}}^{n_x} c_{ij}^{(n)}: \quad i = j\end{aligned} \tag{27}$$

In which:

$$\mathrm{M}(X_i) = \prod_{j=1, j\neq i}^{n} (x_i - x_j) \tag{28}$$

For the second-order or higher-order derivatives $2 \leqslant n \leqslant (N-1)$:

$$\begin{aligned}&c_{ij}^{(n)} = \mathrm{n}\left(c_{ii}^{(n-1)}c_{ij}^{(1)} - \frac{c_{ij}^{(n-1)}}{x_i - x_j}\right), \\ &\mathrm{i},\mathrm{j} = 1,\dots,\mathrm{N} \qquad \mathrm{j} \neq \mathrm{i} \\ &c_{ii}^{(n)} = -\sum_{\substack{j=1\\ j\neq i}}^{n_x} c_{ij}^{(n)},\begin{cases} i = 1,\dots,N \\ n = 1,2,\dots,N-1\end{cases}\end{aligned} \tag{29}$$

In this work, the interpolation points' locations are being taken as Gauss-Lobatto-Chebyshev type as they are considered to be resulting in higher accuracy:

$$x_i = \frac{l}{2}\left(1 - cos\left(\frac{(i-1)}{(n-1)}\pi\right)\right) \quad i = 1,2,3,\dots,n \tag{30}$$

Assuming a harmonic variation for displacements ($[u, w, \emptyset] = [U, W, \emptyset]e^{i\omega t}$) and substituting Eqs. (25) and (26) into Eqs. (24a)-(24c) leads to a set of ordinary differential equations as:

$$\begin{aligned}&\frac{B}{L}\left[\sum_{m=1}^{n} C_{1m}^{(1)}U_m + \frac{1}{2}\left(\sum_{m=1}^{n} C_{1m}^{(1)}W_m\right)^2\right]\\ &+\left(\sum_{m=1}^{n} C_{1m}^{(2)}U_m + \sum_{m=1}^{n} C_{1m}^{(1)}W_m \sum_{m=1}^{n} C_{1m}^{(2)}W_m\right) = 0\end{aligned} \tag{31a}$$

$$\begin{aligned}&\omega^2\mu I_2\left[2\frac{B}{L}\sum_{m=1}^{N} c_{im}^{(1)}\emptyset_m + \sum_{m=1}^{N} c_{im}^{(2)}\emptyset_m + \left(\frac{B}{L}\right)^2\emptyset_i\right]\\ &+A_2\sum_{m=1}^{N} c_{im}^{(2)}\emptyset_m + \frac{B}{L}A_2\sum_{m=1}^{N} c_{im}^{(1)}\emptyset_m\\ &\qquad + A_3\left(\sum_{m=1}^{N} c_{im}^{(1)}W_m - \emptyset_i\right) = 0\end{aligned} \tag{31b}$$

$$\begin{aligned}&A_3\left(\sum_{m=1}^{N} c_{im}^{(2)}W_m - \sum_{m=1}^{N} c_{im}^{(1)}\emptyset_m\right)\\ &+\frac{B}{L}A_3\left(\sum_{m=1}^{N} c_{im}^{(1)}W_m - \emptyset_i\right)\\ &+\left(A_0\left[\sum_{m=1}^{N} c_{im}^{(1)}U_m + \frac{1}{2}\left(\sum_{m=1}^{N} c_{im}^{(1)}W_m\right)^2\right]\right)\left(\sum_{m=1}^{N} c_{im}^{(2)}W_m\right.\\ &\qquad\left. - \mu\sum_{m=1}^{N} c_{im}^{(4)}W_m\right) - \omega^2 I_0 W_i\\ &-\omega^2\mu I_0\left(2\frac{B}{L}\sum_{m=1}^{N} c_{im}^{(1)}W_m + \sum_{m=1}^{N} c_{im}^{(2)}W_m + \left(\frac{B}{L}\right)^2\right) = 0\end{aligned} \tag{31c}$$

where i = 1, 2, . . . , N. A similar approach can be applied to develop the corresponding boundary conditions for a clamped-clamped (CC) BFG microbeam:

$$\begin{aligned}&U_1 = W_1 = \emptyset_1 = 0 \qquad at\ x = 0,\\ &U_N = W_N = \emptyset_N = 0 \qquad at\ x = L\end{aligned} \tag{32}$$

And also, for a simply supported (SS) BFG microbeam:

$$\begin{aligned}&U_1 = W_1 = 0,\\ &\mu\left[-\omega^2 I_0 W_1 + \omega^2 I_2\sum_{m=1}^{N} c_{1m}^{(1)}\emptyset_m + \omega^2\frac{B}{L}I_2\emptyset_1\right.\\ &\qquad - A_0\left(\sum_{m=1}^{N} c_{1m}^{(1)}U_m\right.\\ &\qquad\left.\left. + \frac{1}{2}\left(\sum_{m=1}^{N} c_{1m}^{(1)}W_m\right)^2\right)\sum_{m=1}^{N} c_{1m}^{(2)}W_m\right]\\ &\qquad - A_2\sum_{m=1}^{N} c_{1m}^{(1)}\emptyset_m = 0 \quad at \quad x = 0\end{aligned} \tag{33a}$$

$$\begin{aligned}&U_N = W_N = 0\,,\\ &\mu\left[-\omega^2 I_0 W_N + \omega^2 I_2\sum_{m=1}^{N} c_{Nm}^{(1)}\emptyset_m + w^2\frac{B}{L}I_2\emptyset_N\right.\\ &\qquad - A_0\left(\sum_{m=1}^{N} c_{Nm}^{(1)}U_m\right.\\ &\qquad\left.\left. + \frac{1}{2}\left(\sum_{m=1}^{N} c_{Nm}^{(1)}W_m\right)^2\right)\sum_{m=1}^{N} c_{Nm}^{(2)}W_m\right]\\ &\qquad - A_2\sum_{m=1}^{N} c_{Nm}^{(1)}\emptyset_m = 0 \quad at \quad x = L\end{aligned} \tag{33b}$$

Denoting the mode shape vector of a nonlinear vibration as follows:

$$d = \{\{U_i\}^T, \{W_i\}^T, \{\emptyset_i\}^T\}^T \tag{34}$$

It is possible to provide the matrix form of Eqs. (31a) to (31c) and the relevant boundary conditions Eqs. (32) and (33) as follows:

$$\left(K_L + \frac{1}{2}K_{NL1} + \frac{1}{3}K_{NL2}\right)d - \omega^2 M d = 0 \tag{35}$$

In which, M denotes the mass stiffness matrix, and $\mathrm{K_L}$ denotes the linear stiffness matrix. Moreover, $\mathrm{K_{NL1}}$ and $\mathrm{K_{NL2}}$ are nonlinear stiffness matrices that are linear and quadratic functions in d, respectively. In addition, $\mathrm{K_L}$, $\mathrm{K_{NL1}}$, $\mathrm{K_{NL2}}$ and M are 3×3 symmetric matrices. A direct iterative algorithm proposed by (Kitipornchai *et al*. 2009) can be utilized for solving these equations.

5. Numerical results

This current section of the study includes two subsections. The first subsection focuses on verifying the presented nonlocal model using a comparison to the results of the previous studies. The second subsection deals with the effect of the amplitude ratio, nanobeams length, material distribution, nonlocality, and boundary conditions on the nonlinear frequency of BFG nanobeams through a parametric study.

5.1 Model validation

Three comparison studies are conducted as a means to evaluate the reliability of the presented formulation and the obtained results. First, the results of the current study are compared to the results reported in (Eltaher *et al*. 2012). The linear dimensionless frequencies of the conventional FG nanobeams presented in (Eltaher *et al*. 2012) can be determined when the effects of the FG gradient index along the axial $\mathrm{N_x}$ as well as nonlinear terms are neglected in the current formulation. Tables 1 to 5 present the dimensionless frequencies for SS Timoshenko FG nanobeam with L = 10,000 nm and b = 1000 nm for different amounts of the nonlocal parameter, the slender ratio, and the gradient index. A comparison of the non-dimensionless fundamental

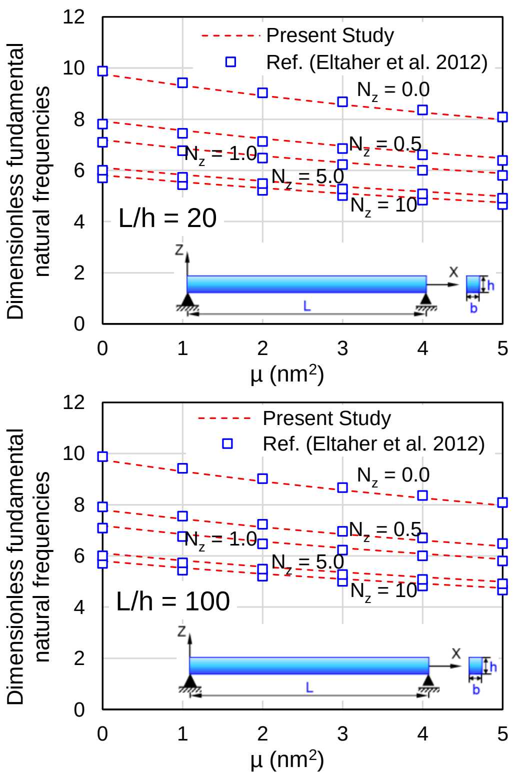

Fig. 2 Comparison of non-dimensionless fundamental natural frequencies of the present study with Eltaher *et al.* (2012)

Table1 Comparison of non-dimensional fundamental natural frequencies $\widehat{\omega}_1=\omega_1 L^2\sqrt{\rho_a A/E_a I}$ of an SS Timoshenko FG nanobeam for $N_z = 0$

L/h	μ (nm²)	Present	Ref. (Eltaher *et al.* 2012)
20	0	9.7611	9.8797
	1	9.3107	9.4238
	2	8.9173	9.0257
	3	8.5700	8.6741
	4	8.2603	8.3607
	5	7.9819	8.0789
50	0	9.7539	9.8724
	1	9.3041	9.4172
	2	8.9122	9.0205
	3	8.5659	8.6711
	4	8.2572	8.3575
	5	7.9795	8.0765
100	0	9.7515	9.8705
	1	9.3032	9.4162
	2	8.9114	9.0197
	3	8.5654	8.6695
	4	8.2568	8.3571
	5	7.9792	8.0762

natural frequencies of the present study and Eltaher *et al.* (2012) are obtained and exhibited in Fig. 2.

Table 2 Comparison of dimensionless fundamental natural frequencies $\widehat{\omega}_1=\omega_1 L^2\sqrt{\rho_a A/E_a I}$ of an SS Timoshenko FG nanobeam for $N_z = 0.5$

L/h	μ (nm²)	Present	Ref. (Eltaher *et al.* 2012)
20	0	7.9231	7.8061
	1	7.5574	7.4458
	2	7.2381	7.1312
	3	6.9560	6.8533
	4	6.7047	6.6057
	5	6.4787	6.3832
50	0	7.9167	7.7998
	1	7.5519	7.4403
	2	7.2338	7.1269
	3	6.9527	6.8525
	4	6.7021	6.6031
	5	6.4768	6.3811
100	0	7.9150	7.7981
	1	7.5512	7.4396
	2	7.2331	7.1263
	3	6.9523	6.8496
	4	6.7018	6.6028
	5	6.4765	6.3808

Table 3 Comparison of dimensionless fundamental natural frequencies $\widehat{\omega}_1=\omega_1 L^2\sqrt{\rho_a A/E_a I}$ of SS Timoshenko FG nanobeam for$N_z = 1$

L/h	μ (nm²)	Present	Ref. (Eltaher *et al.* 2012)
20	0	7.1896	7.0904
	1	6.8577	6.7631
	2	6.5680	6.4774
	3	6.3122	6.2251
	4	6.0841	6.0001
	5	5.8790	5.7979
50	0	7.1843	7.0852
	1	6.8529	6.7583
	2	6.5643	6.4737
	3	6.3093	6.2222
	4	6.0818	5.9979
	5	5.8773	5.7962
100	0	7.1824	7.0833
	1	6.8523	6.7577
	2	6.5637	6.4731
	3	6.3088	6.2217
	4	6.0815	5.9976
	5	5.8771	5.7960

The analytical solutions reported in (Nazemnezhad and Hosseini-Hashemi 2014) are also provided for direct comparison. According to Table 6, the results presented in

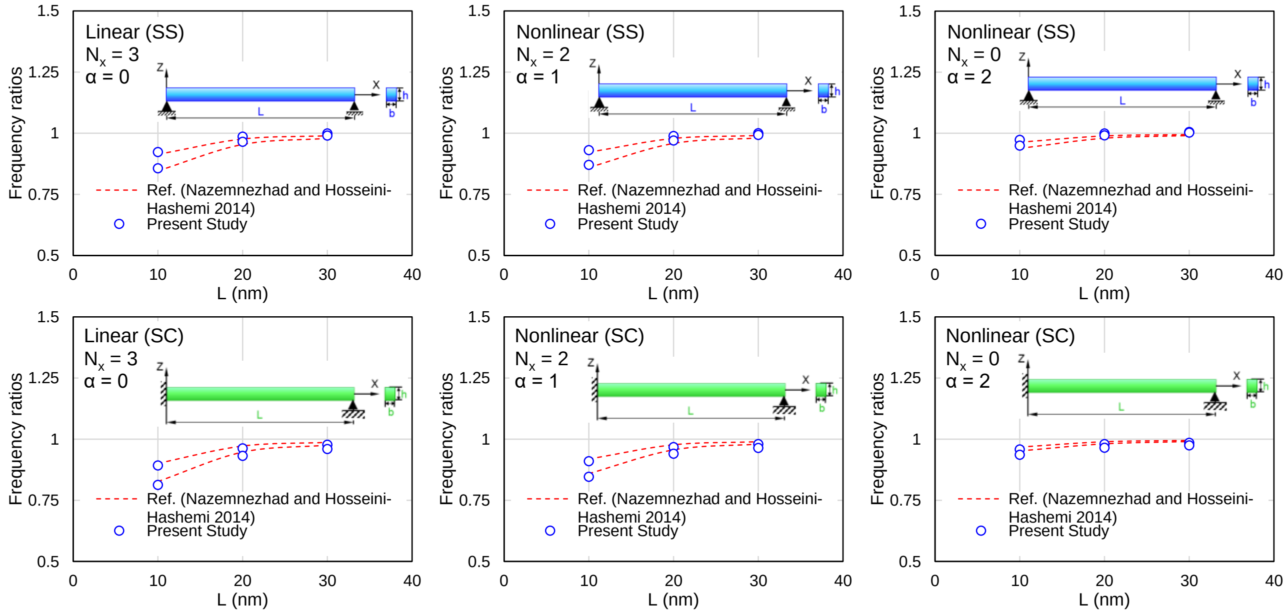

Fig. 3 Comparison of frequency ratios of the present study with Nazemnezhad and Hosseini-Hashemi (2014)

Table 4 Comparison of dimensionless fundamental natural frequencies $\hat{\omega}_1=\omega_1 L^2\sqrt{\rho_a A/E_a I}$ of SS Timoshenko FG nanobeam for$N_z = 5$

L/h	μ (nm^2)	Present	Ref. (Eltaher *et al.* 2012)
20	0	6.1105	6.0025
	1	5.8286	5.7256
	2	5.5824	5.4837
	3	5.3650	5.2702
	4	5.1711	5.0797
	5	4.9969	4.9086
50	0	6.1069	5.9990
	1	5.8247	5.7218
	2	5.5794	5.4808
	3	5.3627	5.2679
	4	5.1694	5.0780
	5	4.9955	4.9072
100	0	6.1049	5.9970
	1	5.8241	5.7212
	2	5.5789	5.4803
	3	5.3623	5.2675
	4	5.1690	5.0777
	5	4.9954	4.9071

Table 5 Comparison of dimensionless fundamental natural frequencies $\hat{\omega}_1=\omega_1 L^2\sqrt{\rho_a A/E_a I}$ of SS Timoshenko FG nanobeam for$N_z = 10$

L/h	μ (nm^2)	Present	Ref. (Eltaher *et al.* 2012)
20	0	5.8085	5.7058
	1	5.5404	5.4425
	2	5.3064	5.2126
	3	5.0997	5.0096
	4	4.9155	4.8286
	5	4.7498	4.6659
50	0	5.8027	5.7001
	1	5.5368	5.4389
	2	5.3035	5.2098
	3	5.0975	5.0074
	4	4.9137	4.8269
	5	4.7485	4.6646
100	0	5.8031	5.7005
	1	5.5362	5.4384
	2	5.3031	5.2094
	3	5.0972	5.0071
	4	4.9135	4.8267
	5	4.7483	4.6644

this study are consistent with those reported in (Nazemnezhad and Hosseini-Hashemi 2014). A comparison of frequency ratios of the SS and SC FG nanobeams the present study and Nazemnezhad and Hosseini-Hashemi (2014) are obtained and exhibited in Fig. 3.

Next, by neglecting the FG power index along axis N_x, the ratio of nonlocal nonlinear frequency-to-classical nonlinear frequency for the SS and simply supported-clamped (SC) FG nanobeams with different values of gradient index N_x, amplitude ratios α, nonlocal parameter μ, and length L are obtained and compared with the Ref. (Nazemnezhad and Hosseini-Hashemi 2014), as shown in Table 6. The results of Ref. (Nazemnezhad and Hosseini-Hashemi 2014) were obtained by the use of Eringen's nonlocal theory according to the Euler–Bernoulli beam theory. Table 6 clearly shows that the current results are

Table 6 Comparison of frequency ratios of the SS and SC FG nanobeams

α	N_x	L (nm)	SS				SC			
			μ(nm²)				μ(nm²)			
			2		4		2		4	
			Ref.[a]	Present	Ref.[a]	Present	Ref.[a]	Present	Ref.[a]	Present
0 (linear)	3	10	0.9139	0.9230	0.8467	0.8569	0.9013	0.8923	0.8267	0.8135
		20	0.9762	0.9860	0.9540	0.9654	0.9724	0.9627	0.9469	0.9317
		30	0.9892	0.9991	0.9788	0.9905	0.9874	0.9775	0.9753	0.9597
1 (Nonlinear)	0	10	0.9293	0.9386	0.8754	0.8859	0.9202	0.9110	0.8625	0.8487
		20	0.9803	0.9901	0.9621	0.9736	0.9774	0.9676	0.9567	0.9414
		30	0.9911	1.0010	0.9824	0.9942	0.9897	0.9798	0.9798	0.9641
	1	10	0.9247	0.9339	0.8659	0.8763	0.9205	0.9113	0.8625	0.8487
		20	0.9792	0.9890	0.9599	0.9714	0.9775	0.9677	0.9569	0.9416
		30	0.9906	1.0005	0.9815	0.9933	0.9898	0.9799	0.9799	0.9642
	2	10	0.9221	0.9313	0.8607	0.8710	0.9192	0.9100	0.8598	0.8460
		20	0.9786	0.9884	0.9585	0.9700	0.9772	0.9674	0.9562	0.9409
		30	0.9903	1.0002	0.9809	0.9927	0.9896	0.9797	0.9796	0.9639
	3	10	0.9221	0.9313	0.8608	0.8711	0.9209	0.9117	0.8632	0.8494
		20	0.9785	0.9883	0.9585	0.9700	0.9776	0.9678	0.9571	0.9418
		30	0.9903	1.0002	0.9809	0.9927	0.9898	0.9799	0.9800	0.9643
2 (Nonlinear)	0	10	0.9631	0.9727	0.9379	0.9492	0.9676	0.9579	0.9519	0.9367
		20	0.9893	0.9992	0.9797	0.9915	0.9899	0.9800	0.9812	0.9655
		30	0.9951	1.0051	0.9905	1.0024	0.9953	0.9853	0.9909	0.9750
	1	10	0.9491	0.9586	0.9087	0.9196	0.9680	0.9583	0.9509	0.9357
		20	0.9860	0.9959	0.9729	0.9846	0.9901	0.9802	0.9816	0.9659
		30	0.9936	1.0035	0.9875	0.9994	0.9954	0.9854	0.9912	0.9753
	2	10	0.9412	0.9506	0.8929	0.9036	0.9639	0.9543	0.9426	0.9275
		20	0.9840	0.9938	0.9689	0.9805	0.9891	0.9792	0.9796	0.9639
		30	0.9928	1.0027	0.9857	0.9975	0.9950	0.9851	0.9903	0.9745
	3	10	0.9413	0.9507	0.8936	0.9043	0.9700	0.9603	0.9545	0.9392
		20	0.9840	0.9938	0.9689	0.9805	0.9907	0.9808	0.9827	0.9670
		30	0.9927	1.0026	0.9857	0.9975	0.9957	0.9857	0.9916	0.9757

[a]Nazemnezhad and Hosseini-Hashemi (2014)

consistent with those reported in (Nazemnezhad and Hosseini-Hashemi 2014).

With the aim of further validating the precision of the proposed formulation, the ratio of classical nonlinear frequency to the classical linear frequency, obtained for isotropic macrobeams with SS boundary conditions, are compared with those reported in (Lestari and Hanagud 2001, Singh *et al*. 1990) for various amounts of the amplitude ratio ($\alpha = 1, 2$ and 3), as shown in Table 7. Note that the frequency of the isotropic macrobeams can be obtained by substituting $\mu = 0$, $N_x = 0$ and $N_z = 0$ in the current formulation. The results reported (Lestari and Hanagud 2001, Singh *et al*. 1990) were obtained by use of the exact solution and the Ritz–Galerkin method, respectively. According to the data presented in Table 7, the current results are consistent with those reported in (Lestari and Hanagud 2001, Singh *et al*. 1990).

5.2 Parametric results

This section deals with the investigation on effects of amplitude ratio, nanobeam length, material distribution, nonlocal parameter, and boundary conditions on the nonlinear frequency of a BFG nanobeam with 100 nm thickness and 10 nm width. The materials of the lower and upper surfaces of the BFG nanobeam are identical to the those used in (Nejad and Hadi 2016b).

The findings are provided based on the nonlinear frequency ratio ($Fr = \bar{\omega}/\overline{\omega_l}$) and the dimensionless nonlinear frequency ($\bar{\omega} = \omega L\sqrt{I/A}$), where $\bar{\omega}_L$ denotes the non-dimensional nonlinear frequency in cases where the nonlocal parameter is set to 0.
The changes in the non-dimensional nonlinear frequency $\bar{\omega}$ versus gradient parameters N_x and N_z have been shown in Fig. 4 for CC and SS boundary conditions, when $L/h = 5$, $\alpha = 1$ and $\mu = 2\ nm^2$.

Table 7 Comparing the nonlinear frequency ratio for an SS isotropic macrobeam

α	Present	Ref. (Lestari and Hanagud 2001)	Ref. (Singh *et al*. 1990)
1	1.0937	1.0892	1.0897
2	1.3750	1.3178	1.3229
3	1.8438	1.6257	1.6394

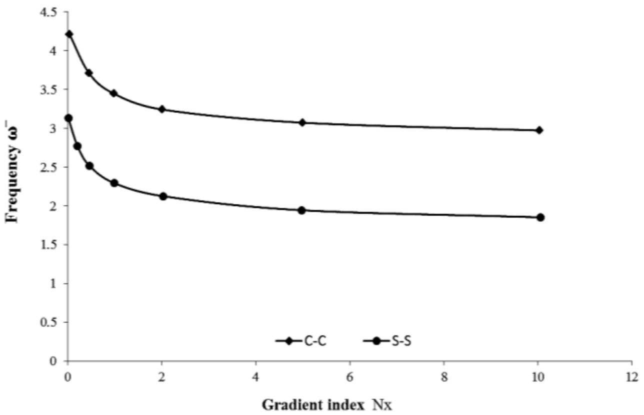

(a)

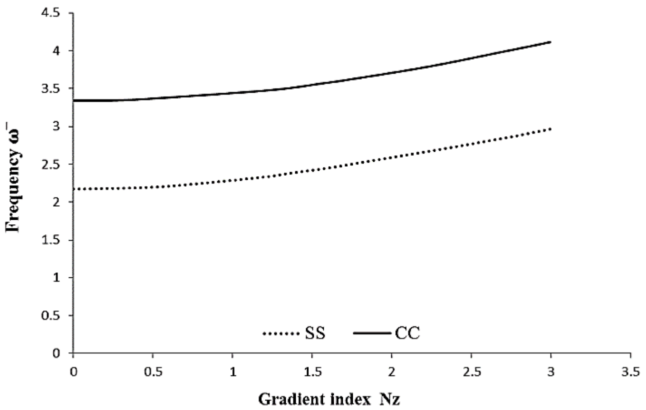

(b)

Fig. 4 Changes of dimensionless nonlinear frequency $\overline{\omega}$ for beam with CC and SS boundary conditions versus a) gradient parameter N_x (b) gradient parameter N_z

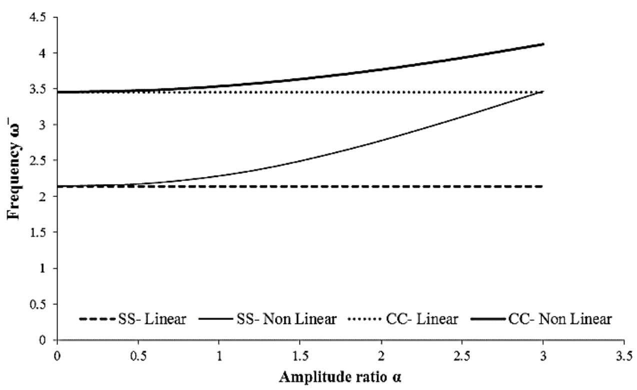

Fig. 5 Changes in the non-dimensional linear and nonlinear frequencies of SS and CC microbeam versus amplitude ratio α

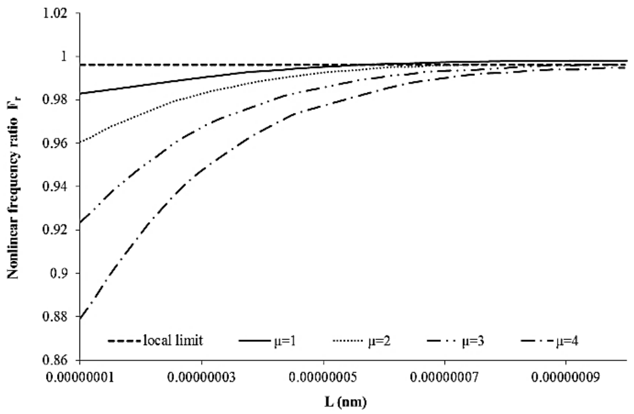

(a)

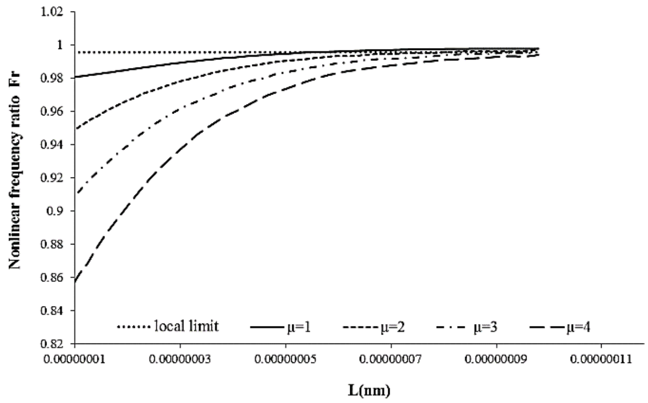

(b)

Fig. 6 Variations of the nonlinear frequency ratio Fr versus nanobeam length L for various amounts of nonlocal parameter μ: (a) SS microbeam, and (b) CC microbeam

Based on the results, N_x and N_z affect the dimensionless nonlinear frequency $\overline{\omega}$ significantly. It is seen that for both boundary conditions, the dimensionless nonlinear frequency increases by decreasing N_x and increasing N_z. This issue can be justified by the observation that the volume fraction of harder material and as a consequence, nanobeam stiffness, increase as N_x decreases and N_z increases.

Next, the changes in the non-dimensional linear and nonlinear frequencies versus the amplitude ratio α are investigated. The variations are plotted in Fig. 5. For CC and SS boundary conditions when $N_x = 1$, $N_z = 1$, $L/h = 5$ and $\mu = 2\,nm^2$.

According to the figure, nonlinear frequency increases as the amplitude ratio increases because of hardening spring behavior. It was also found that the nonlinear vibration frequency is greater than the linear vibration frequency for all values of α. The reason is that considering geometric nonlinearity results in the stiffness of nanobeam to increase. Besides, the difference between the dimensionless linear frequency and nonlinear frequency for CC nanobeam is smaller than that of SS nanobeam. It should be mentioned that the impact of geometric nonlinearity on the non-dimensional nonlinear frequency in the C-C nanobeam could be neglected for $0 < \alpha < 1.5$.

Fig. 6 represents the impacts of variations in nanobeam length on the nonlinear frequency ratio Fr of the nanobeam with SS and CC boundary condition for the constant values of $\alpha = 4$, $N_z = 1$ and $N_x = 1$ and various values of $\mu = 1\ \mathrm{nm}^2$, $2\ \mathrm{nm}^2$, $3\ \mathrm{nm}^2$ and $4\ \mathrm{nm}^2$. According to the figure, the nonlinear frequency ratio increments as the value of μ increments. By increasing the length of nanobeam, the dependency of the nonlinear frequency ratio on μ decreases. for example, the nonlinear frequency ratio increases by 7 %, 5%, and 2 % for $L = 10\ \mathrm{nm}$, $20\ \mathrm{nm}$, and $40\ \mathrm{nm}$ as the μ increases from 3 to 4. Also, it is clear from Fig.4 that when L increases, the crease of F_r will occur; for L = 90 nm, the nonlinear frequency estimated according to the nonlocal theory is almost equal to one estimated according to the nonlinear classical theory.

6. Conclusions

In conclusion, this text presents a detailed theoretical formulation for the analysis of bi-directional functionally graded (BFG) nanobeams using Eringen's nonlocal theory and the Timoshenko beam theory. The key points covered in this text include the theoretical background, functionally-graded materials, and the derivation of governing equations and boundary conditions for BFG nanobeams. Additionally, the text discusses the use of the numerical differential quadrature method (DQM) to solve the resulting nonlinear equations of motion. Furthermore, the text addresses model validation by comparing the non-dimensional fundamental natural frequencies of BFG nanobeams with the results from a previous study. This validation demonstrates the reliability of the presented formulation. In this comprehensive study has presented a detailed theoretical formulation for the mechanical behavior of bi-directional functionally graded (BFG) nanobeams. The key contributions and findings of this research can be summarized as follows:

• The study established a rigorous theoretical framework for understanding the mechanical characteristics of BFG nanobeams, emphasizing the changes in material properties along both their length and thickness directions. This approach allowed for a more accurate representation of BFG nanobeams compared to previous studies that primarily focused on functionally graded (FG) micro/ nanobeams.

• The material properties of BFG nanobeams were described using mathematical equations that consider the variations in Young's modulus and mass density as functions of both the position along the beam and the gradient parameters. These equations provide a versatile means to model the material properties of BFG nanomaterials, accounting for both ceramic and metallic constituents.

• The research incorporated Eringen's nonlocal theory, which accounts for the influence of strain at any point within the material domain. This addition allowed for a more accurate representation of stress distribution in BFG nanobeams and considered the effects of nonlocal parameters on the mechanical behavior.

• The presented formulation was validated by comparing the results of the current study to those of previous research, demonstrating its accuracy and reliability in predicting the fundamental natural frequencies of BFG nanobeams.

• The research conducted a parametric study to investigate the impact of various parameters, such as amplitude ratio, nanobeam length, material distribution, nonlocality, and boundary conditions, on the nonlinear frequency of BFG nanobeams. This analysis offered valuable insights into the sensitivity of BFG nanobeams to different influencing factors.

• The main findings of the study can be summarized as follows:

• Gradient parameters N_z and N_x significantly impact on the dimensionless nonlinear frequency $\bar{\omega}_L$ of BFG nanobeams. Thus, the desired value of $\bar{\omega}_L$ can be approached using the appropriate gradient parameters N_z and N_x.

• The nonlinear vibration frequency is higher than the linear vibration frequency, for all values of α.

• Because of hardening spring behavior, the nonlinear frequency increments when parameter α increments.

• The difference between the dimensionless linear frequency and the nonlinear frequency for CC nanobeam is smaller than that of SS nanobeam. For $0 < \alpha < 1.5$, the impact of the geometric nonlinearity on the non-dimensional nonlinear frequency in the CC nanobeam could be neglected.

• The nonlinear frequency ratio increments as the value of μ is incremented. By increasing the length of nanobeam, dependency of the nonlinear frequency ratio on μ decreases.

• With increasing nanobeam length L, the crease of Fr will occur. In the length rage of from$10\ nm$-$30\ nm$, the rate of increase in the nonlinear frequency ratio was high.

References

Ahouel, M., Houari, M.S.A., Bedia, E.A.A. and Tounsi, A. (2016), "Size-dependent mechanical behavior of functionally graded trigonometric shear deformable nanobeams including neutral surface position concept", *Steel Compos. Struct.*, **20**(5), 963-981. https://doi.org/10.12989/scs.2016.20.5.963.

Almitani, K.H., Eltaher, M.A., Abdelrahman, A.A. and Abd-El-Mottaleb, H.E. (2021), "Finite element based stress and vibration analysis of axially functionally graded rotating beams", *Struct. Eng. Mech.*, **79**(1), 23-33. https://doi.org/10.12989/sem.2021.79.1.023.

Amar, L.H.H., Kaci, A. and Tounsi, A. (2017), "On the size-dependent behavior of functionally graded micro-beams with porosities", *Struct. Eng. Mech.*, **64**(5), 527. https://doi.org/10.12989/SCS.2017.64.5.527.

Ansari, R., Gholami, R. and Sahmani, S. (2011), "Free vibration analysis of size-dependent functionally graded microbeams based on the strain gradient Timoshenko beam theory", *Compos. Struct.*, **94**(1), 221-228. https://doi.org/10.1016/j.compstruct.2011.06.024.

Ansari, R., Pourashraf, T. and Gholami, R. (2015), "An exact solution for the nonlinear forced vibration of functionally graded nanobeams in thermal environment based on surface elasticity theory", *Thin-Walled Struct.*, **93**, 169-176.

https://doi.org/10.1016/j.tws.2015.03.013.

Asghari, M., Rahaeifard, M., Kahrobaiyan, M.H. and Ahmadian, M.T. (2011), "The modified couple stress functionally graded Timoshenko beam formulation", *Mater. Des.*, **32**(3), 1435-1443. https://doi.org/10.1016/j.matdes.2010.08.046.

Atmane, H.A., Tounsi, A., Bernard, F. and Mahmoud, S.R. (2015), "A computational shear displacement model for vibrational analysis of functionally graded beams with porosities", *Steel Compos. Struct.*, **19**(2), 369-384. https://doi.org/10.12989/scs.2015.19.2.369.

Aydogdu, M., Arda, M. and Filiz, S. (2018), "Vibration of axially functionally graded nano rods and beams with a variable nonlocal parameter", *Adv. Nano Res.*, **6**(3), 257-278. https://doi.org/10.12989/anr.2018.6.3.257.

Aydogdu, M. and Taskin, V. (2007), "Free vibration analysis of functionally graded beams with simply supported edges", *Mater. Des.*, **28**(5), 1651-1656. https://doi.org/10.1016/j.matdes.2006.02.007.

Azandariani, M.G., Gholami, M. and Nikzad, A. (2022), "Eringen's nonlocal theory for non-linear bending analysis of BGF Timoshenko nanobeams", *Adv. Nano Res.*, **12**(1), 37. https://doi.org/10.12989/ANR.2022.12.1.037.

Belarbi, M.O., Houari, M.S.A., Daikh, A.A., Garg, A., Merzouki, T., Chalak, H.D. and Hirane, H. (2021), "Nonlocal finite element model for the bending and buckling analysis of functionally graded nanobeams using a novel shear deformation theory", *Compos. Struct.*, Elsevier Ltd, **264**, 113712. https://doi.org/10.1016/j.compstruct.2021.113712.

Bennai, R., Atmane, H.A. and Tounsi, A. (2015), "A new higher-order shear and normal deformation theory for functionally graded sandwich beams", *Steel Compos. Struct.*, Techno Press, **19**(3), 521-546. https://doi.org/10.12989/scs.2015.19.3.521.

Chaht, F.L., Kaci, A., Houari, M.S.A., Tounsi, A., Bég, O.A. and Mahmoud, S.R. (2015), "Bending and buckling analyses of functionally graded material (FGM) size-dependent nanoscale beams including the thickness stretching effect", *Steel Compos. Struct.*, **18**(2), 425-442. https://doi.org/10.12989/scs.2015.18.2.425.

Daikh, A.A., Houari, M.S.A. and Eltaher, M.A. (2021), "A novel nonlocal strain gradient Quasi-3D bending analysis of sigmoid functionally graded sandwich nanoplates", *Compos. Struct.*, **262**, 113347. https://doi.org/10.1016/j.compstruct.2020.113347.

Dergachova, N.V. and Zou, G. (2021), "Dynamic response of functionally graded plates with a porous middle layer under time-dependent load", *Comput. Concr.*, **27**(3), 269-282. https://doi.org/10.12989/cac.2021.27.3.269.

Ebrahimi, F. and Barati, M.R. (2018), "Stability analysis of functionally graded heterogeneous piezoelectric nanobeams based on nonlocal elasticity theory", *Adv. Nano Res.*, **6**(2), 93-112. https://doi.org/10.12989/anr.2018.6.2.093.

Ebrahimi, F. and Haghi, P. (2018), "Elastic wave dispersion modelling within rotating functionally graded nanobeams in thermal environment", *Adv. Nano Res.*, **6**(3), 201-217. https://doi.org/10.12989/anr.2018.6.3.201.

Elmascri, S., Bessaim, A., Taleb, O., Houari, M.S.A., Mohamed, S., Bernard, F. and Tounsi, A. (2020), "A novel hyperbolic plate theory including stretching effect for free vibration analysis of advanced composite plates in thermal environments" *Struct. Eng. Mech.*, **75**(2), 193-209. https://doi.org/10.12989/SCS.2020.75.2.193.

Eltaher, M.A., Alshorbagy, A.E. and Mahmoud, F.F. (2013a), "Determination of neutral axis position and its effect on natural frequencies of functionally graded macro/nanobeams", *Compos. Struct.*, **99**, 193-201. https://doi.org/10.1016/j.compstruct.2012.11.039.

Eltaher, M.A., Emam, S.A. and Mahmoud, F.F. (2012), "Free vibration analysis of functionally graded size-dependent nanobeams", *Appl. Math. Comput.*, **218**(14), 7406-7420. https://doi.org/10.1016/j.amc.2011.12.090.

Eltaher, M. A., Emam, S. A. and Mahmoud, F. F. (2013b), "Static and stability analysis of nonlocal functionally graded nanobeams", *Compos. Struct.*, **96**, 82-88. https://doi.org/10.1016/j.compstruct.2012.09.030.

Eringen, A.C. (1983), "On differential equations of nonlocal elasticity and solutions of screw dislocation and surface waves", *J. Appl. Phys.*, **54**(9), 4703-4710. https://doi.org/10.1063/1.332803.

Gao, Y., Xiao, W. and Zhu, H. (2019), "Nonlinear thermal buckling of bi-directional functionally graded nanobeams", *Struct. Eng. Mech.*, **71**(6), 669. https://doi.org/10.12989/SEM.2019.71.6.669.

Gholami, M., Gorji Azandariani, M., Najat Ahmed, A. and Abdolmaleki, H. (2023), "Proposing a dynamic stiffness method for the free vibration of bi-directional functionally-graded Timoshenko nanobeams", *Adv. Nano Res.*, **14**(2), 127-139. https://doi.org/https://doi.org/10.12989/anr.2023.14.2.127.

Ghorbanpour Arani, A., Hashemian, M. and Kolahchi, R. (2013), "Nonlocal Timoshenko beam model for dynamic stability of double-walled boron nitride nanotubes conveying nanoflow", *Proceedings of the Institution of Mechanical Engineers, Part N: Journal of Nanoengineering and Nanosystems*, **229**(1), 2-16. https://doi.org/10.1177/1740349913513449.

Gorji Azandariani, M., Gholami, M. and Zare, E. (2022), "Development of spectral element method for free vibration of axially-loaded functionally-graded beams using the first-order shear deformation theory", *Eur. J. Mech. A Solids*, **96**, 104759. https://doi.org/10.1016/j.euromechsol.2022.104759.

Hashemian, M., Falsafioon, M., Pirmoradian, M. and Toghraie, D. (2020), "Nonlocal dynamic stability analysis of a Timoshenko nanobeam subjected to a sequence of moving nanoparticles considering surface effects", *Mech. Mater.*, Elsevier, **148**, 103452. https://doi.org/10.1016/J.MECHMAT.2020.103452.

Hashemian, M., Foroutan, S. and Toghraie, D. (2019), "Comprehensive beam models for buckling and bending behavior of simple nanobeam based on nonlocal strain gradient theory and surface effects", *Mech. Mater.*, **139**, 103209. https://doi.org/10.1016/J.MECHMAT.2019.103209.

Hirane, H., Belarbi, M.O., Houari, M.S.A. and Tounsi, A. (2021), "On the layerwise finite element formulation for static and free vibration analysis of functionally graded sandwich plates", *Eng. Comput.*, 1-29. https://doi.org/10.1007/s00366-020-01250-1.

Jia, X.L., Ke, L.L., Feng, C.B., Yang, J. and Kitipornchai, S. (2015), "Size effect on the free vibration of geometrically nonlinear functionally graded micro-beams under electrical actuation and temperature change", *Compos. Struct.*, **133**, 1137-1148. https://doi.org/10.1016/j.compstruct.2015.08.044.

Karami, B. and Janghorban, M. (2019), "On the dynamics of porous nanotubes with variable material properties and variable thickness", *Int. J. Eng. Sci.*, **136**, 53-66. https://doi.org/10.1016/j.ijengsci.2019.01.002.

Karami, B. and Janghorban, M. (2020), "On the mechanics of functionally graded nanoshells", *Int. J. Eng. Sci.*, **153**, 103309. https://doi.org/10.1016/j.ijengsci.2020.103309.

Karami, B., Janghorban, M. and Rabczuk, T. (2019a), "Static analysis of functionally graded anisotropic nanoplates using nonlocal strain gradient theory", *Compos. Struct.*, **227**, 111249. https://doi.org/10.1016/j.compstruct.2019.111249.

Karami, B., Janghorban, M. and Rabczuk, T. (2019b), "Analysis of elastic bulk waves in functionally graded triclinic nanoplates using a quasi-3D bi-Helmholtz nonlocal strain gradient model", *Eur. J. Mech. A Solids*, **78**, 103822. https://doi.org/10.1016/j.euromechsol.2019.103822.

Karami, B., Janghorban, M. and Rabczuk, T. (2020), "Dynamics of two-dimensional functionally graded tapered Timoshenko nanobeam in thermal environment using nonlocal strain gradient theory", *Compos. Part B Eng.*, **182**, 107622. https://doi.org/10.1016/j.compositesb.2019.107622.

Karami, B., Shahsavari, D. and Janghorban, M. (2018), "A comprehensive analytical study on functionally graded carbon nanotube-reinforced composite plates", *Aerosp. Sci. Technol.*, **82-83**, 499-512. https://doi.org/10.1016/j.ast.2018.10.001.

Karami, B., Shahsavari, D., Janghorban, M. and Li, L. (2019c), "Influence of homogenization schemes on vibration of functionally graded curved microbeams", *Compos. Struct.*, **216**, 67-79. https://doi.org/10.1016/j.compstruct.2019.02.089.

Ke, L.L., Wang, Y.S., Yang, J. and Kitipornchai, S. (2012), "Nonlinear free vibration of size-dependent functionally graded microbeams", *Int. J. Eng. Sci.*, **50**(1), 256-267. https://doi.org/10.1016/j.ijengsci.2010.12.008.

Kim, D.H., Chang, Y.S. and Jhung, M.J. (2014), "Numerical study on fluid flow by hydrodynamic loads in reactor internals", *Struct. Eng. Mech.*, **51**(6), 1005-1016. https://doi.org/10.12989/sem.2014.51.6.1005.

Kitipornchai, S., Ke, L.L., Yang, J. and Xiang, Y. (2009), "Nonlinear vibration of edge cracked functionally graded Timoshenko beams", *J. Sound Vib.*, **324**(3-5), 962-982. https://doi.org/10.1016/j.jsv.2009.02.023.

Lestari, W. and Hanagud, S. (2001), "Nonlinear vibration of buckled beams: some exact solutions", *Int. J. Solids Struct.*, **38**(26-27), 4741-4757. https://doi.org/10.1016/S0020-7683(00)00300-0.

Li, L. and Hu, Y. (2016), "Nonlinear bending and free vibration analyses of nonlocal strain gradient beams made of functionally graded material", *Int. J. Eng. Sci.*, **107**, 77-97. https://doi.org/10.1016/j.ijengsci.2016.07.011.

Li, L., Li, X. and Hu, Y. (2016), "Free vibration analysis of nonlocal strain gradient beams made of functionally graded material", *Int. J. Eng. Sci.*, **102**, 77-92. https://doi.org/10.1016/j.ijengsci.2016.02.010.

Lim, C.W., Zhang, G. and Reddy, J.N. (2015), "A higher-order nonlocal elasticity and strain gradient theory and its applications in wave propagation", *J. Mech. Phys. Solids*, **78**, 298-313. https://doi.org/10.1016/j.jmps.2015.02.001.

Luat, D. T., Thom, D. Van, Thanh, T. T., Minh, P. Van, Ke, T. Van, and Vinh, P. Van. (2021), "Mechanical analysis of bi-functionally graded sandwich nanobeams", *Adv. Nano Res.*, **11**(1), 055. https://doi.org/10.12989/ANR.2021.11.1.055.

Meradjah, M., Kaci, A., Houari, M.S.A., Tounsi, A. and Mahmoud, S.R. (2015), "A new higher order shear and normal deformation theory for functionally graded beams", *Steel Compos. Struct.*, **18**(3), 793-809. https://doi.org/10.12989/scs.2015.18.3.793.

Moatallebi, M.A., Hashemian, M., Eftekhari, S.A., Toghraie, D. and Pirmoradian, M. (2022), "Supersonic flutter and free vibration features of functionally graded material nanobeams incorporating surface effects", *Waves Random Complex Med.*, 1-36. https://doi.org/10.1080/17455030.2022.2159092.

Nazemnezhad, R. and Hosseini-Hashemi, S. (2014), "Nonlocal nonlinear free vibration of functionally graded nanobeams", *Compos. Struct.*, **110**, 192-199. https://doi.org/10.1016/j.compstruct.2013.12.006.

Nejad, M.Z. (2016), "Hadi A. Eringen's non-local elasticity theory for bending analysis of bi-directional functionally graded Euler-Bernoulli nano-beams", *Int J Eng Sci*, **106**, 1-9.

Nejad, M.Z. and Hadi, A. (2016a), "Non-local analysis of free vibration of bi-directional functionally graded Euler-Bernoulli nano-beams", *Int. J. Eng. Sci.*, **105**, 1-11. https://doi.org/10.1016/j.ijengsci.2016.04.011.

Nejad, M.Z. and Hadi, A. (2016b), "Eringen's non-local elasticity theory for bending analysis of bi-directional functionally graded Euler-Bernoulli nano-beams", *Int. J. Eng. Sci.*, **106**, 1-9. https://doi.org/10.1016/j.ijengsci.2016.05.005.

Nejad, M.Z., Hadi, A., Omidvari, A. and Rastgoo, A. (2018), "Bending analysis of bi-directional functionally graded Euler-Bernoulli nano-beams using integral form of Eringen's non-local elasticity theory", *Struct. Eng. Mech.*, **67**(4), 417-425. https://doi.org/10.12989/sem.2018.67.4.417.

Nejad, M.Z., Hadi, A. and Rastgoo, A. (2016), "Buckling analysis of arbitrary two-directional functionally graded Euler-Bernoulli nano-beams based on nonlocal elasticity theory", *Int. J. Eng. Sci.*, **103**, 1-10. https://doi.org/10.1016/j.ijengsci.2016.03.001.

Nejadi, M.M. and Mohammadimehr, M. (2020), "Analysis of a functionally graded nanocomposite sandwich beam considering porosity distribution on variable elastic foundation using DQM: Buckling and vibration behaviors", *Comput. Concr.*, **25**(3), 215-224. https://doi.org/10.12989/cac.2020.25.3.215.

Niknam, H., Fallah, A. and Aghdam, M.M. (2014), "Nonlinear bending of functionally graded tapered beams subjected to thermal and mechanical loading", *Int. J. Non. Linear. Mech.*, **65**, 141-147. https://doi.org/10.1016/j.ijnonlinmec.2014.05.011.

Rabhi, M., Benrahou, K.H., Kaci, A., Houari, M.S.A., Bourada, F., Bousahla, A.A., Tounsi, A., Bedia, E.A.A., Mahmoud, S.R. and Tounsi, A. (2020), "A new innovative 3-unknowns hsdt for buckling and free vibration of exponentially graded sandwich plates resting on elastic foundations under various boundary conditions", *Geomech. Eng.*, **22**(2), 119-132. https://doi.org/10.12989/gae.2020.22.2.119.

Rahmani, O. and Pedram, O. (2014), "Analysis and modeling the size effect on vibration of functionally graded nanobeams based on nonlocal Timoshenko beam theory", *Int. J. Eng. Sci.*, **77**, 55-70. https://doi.org/10.1016/j.ijengsci.2013.12.003.

Saffari, S., Hashemian, M. and Toghraie, D. (2017), "Dynamic stability of functionally graded nanobeam based on nonlocal Timoshenko theory considering surface effects", *Phys. B Condens. Matter*, **520**, 97-105. https://doi.org/10.1016/J.PHYSB.2017.06.029.

Saidi, H., Houari, M.S.A., Tounsi, A. and Bedia, E.A.A. (2013), "Thermo-mechanical bending response with stretching effect of functionally graded sandwich plates using a novel shear deformation theory", *Steel Compos. Struct.*, **15**(2), 221-245. https://doi.org/10.12989/scs.2013.15.2.221.

Sanjay Anandrao, K., Gupta, R.K., Ramchandran, P. and Venkateswara Rao, G. (2012), "Non-linear free vibrations and post-buckling analysis of shear flexible functionally graded beams", *Struct. Eng. Mech.*, **44**(3), 339-361. https://doi.org/10.12989/sem.2012.44.3.339.

Setoodeh, A.R. and Rezaei, M. (2017), "Large amplitude free vibration analysis of functionally graded nano/micro beams on nonlinear elastic foundation", *Struct. Eng. Mech.*, **61**(2), 209-220. https://doi.org/10.12989/sem.2017.61.2.209.

Şimşek, M. (2014), "Large amplitude free vibration of nanobeams with various boundary conditions based on the nonlocal elasticity theory", *Compos. Part B Eng.*, **56**, 621-628. https://doi.org/10.1016/j.compositesb.2013.08.082.

Şimşek, M. (2016), "Nonlinear free vibration of a functionally graded nanobeam using nonlocal strain gradient theory and a novel Hamiltonian approach", *Int. J. Eng. Sci.*, **105**, 12-27. https://doi.org/10.1016/j.ijengsci.2016.04.013.

Simsek, M. and Yurtcu, H.H. (2013), "Analytical solutions for bending and buckling of functionally graded nanobeams based on the nonlocal Timoshenko beam theory", *Compos. Struct.*, **97**, 378-386. https://doi.org/10.1016/j.compstruct.2012.10.038.

Sina, S.A., Navazi, H.M. and Haddadpour, H. (2009), "An analytical method for free vibration analysis of functionally graded beams", *Mater. Des.*, **30**(3), 741-747. https://doi.org/10.1016/j.matdes.2008.05.015.

Singh, G., Sharma, A.K. and Venkateswara Rao, G. (1990), "Large-amplitude free vibrations of beams—A discussion on various formulations and assumptions", *J. Sound Vib*., **142**(1), 77-85. https://doi.org/10.1016/0022-460X(90)90583-L.

Su, H. and Banerjee, J.R. (2015), "Development of dynamic stiffness method for free vibration of functionally graded Timoshenko beams", *Comput. Struct*., **147**, 107-116. https://doi.org/10.1016/j.compstruc.2014.10.001.

Xu, X., Karami, B. and Janghorban, M. (2021), "On the dynamics of nanoshells", *Int. J. Eng. Sci*., **158**, 103431. https://doi.org/10.1016/j.ijengsci.2020.103431.

Yang, F., Chong, A.C.M., Lam, D.C.C. and Tong, P. (2002), "Couple stress based strain gradient theory for elasticity", *Int. J. Solids Struct*., **39**(10), 2731-2743. https://doi.org/10.1016/S0020-7683(02)00152-X.

Zenkour, A.M. and Abouelregal, A.E. (2015), "Thermoelastic interaction in functionally graded nanobeams subjected to time-dependent heat flux", *Steel Compos. Struct*., **18**(4), 909-924. https://doi.org/10.12989/scs.2015.18.4.909.

Zhou, J., Moradi, Z., Safa, M. and Khadimallah, M.A. (2022), "Intelligent modeling to investigate the stability of a two-dimensional functionally graded porosity-dependent nano-beam", *Comput. Concr*., Techno-Press, **30**(2), 85-97. https://doi.org/10.12989/cac.2022.30.2.085.

Zidi, M., Houari, M.S.A., Tounsi, A., Bessaim, A. and Mahmoud, S.R. (2017), "A novel simple two-unknown hyperbolic shear deformation theory for functionally graded beams", *Struct. Eng. Mech*., **64**(2), 145-153. https://doi.org/10.12989/sem.2017.64.2.145.

CC